

**MICROCHANNEL HEAT SINKS FOR COOLING HIGH HEAT FLUX
ELECTRONIC DEVICES—ANALYSIS WITH SINGLE AND
TWO PHASE FLOWS**

by

PRADEEP GANESH HEGDE

**Thesis submitted in fulfilment of the
requirements for the degree of
Doctor of Philosophy**

June 2006

ACKNOWLEDGEMENTS

I express my profound sense of gratitude to my technical supervisors Prof. Madya Dr. Mohd. Zulkifly Abdullah and Prof. Ahmad Yussof Hassan for their excellent guidance, technical discussions, personal care and continuous encouragement. It was indeed a great experience working with them.

My heartfelt thanks to the Dean of the School Prof. Madya Dr. Zaidi Mohd. Riphin for his persistent support.

I thank Prof. K.N. Seetharamu who being my guide for the former half of my work provided beneficial technical directions and innovative ideas. My sincere gratitude to Dr. Abdul Quadir, Dr. Aswatha Narayana and Prof. Madya Dr. Zainal Alimuddin for their technical as well as personal help.

My sincere thanks to Mr. N.S. Krishnamurthy, Prof. Krishnan Murugesan, Prof. R. Venkatram and Prof. M.S. Rajagopal all of whose support were of personal importance during the work.

I owe my deepest sense of gratitude to my parents, as nothing would have been really possible without their support, encouragement and sacrifice. I thank my wife Deepa for giving me immense love and motivation that helped me expedite my work. I also express my gratitude to my sister, brother in law and my dear nephew Shreyas for their love and encouragement.

I extend my profound sense of gratitude towards Universiti Sains Malaysia for supporting my work with the IRPA grant.

Pradeep G. Hegde

TABLE OF CONTENTS

	Page
ACKNOWLEDGEMENTS	ii
TABLE OF CONTENTS	iii
LIST OF TABLES	vii
LIST OF FIGURES	ix
LIST OF SYMBOLS	xix
LIST OF ABBREVIATIONS	xxi
LIST OF APPENDICES	xxii
LIST OF PUBLICATIONS & SEMINARS	xxii
ABSTRAK	xxiv
ABSTRACT	xxvi
CHAPTER ONE : INTRODUCTION	1
1.0 Application of Microchannel Heat Sinks for Microelectronics Cooling	1
1.1 Literature Review	9
1.1.1 Microchannel Heat Sink Analysis with Single- Phase Flow	9
1.1.2 Use of Nanofluids as Coolants	13
1.1.3 Microchannel Heat Sink Analysis with Two-Phase Flow	14
1.2 Objectives of The Present Work	19
1.3 Overview of the Present Work and Organization of the Thesis	20
CHAPTER TWO : FINITE ELEMENT MODEL FOR THERMAL ANALYSIS OF MICROCHANNEL HEAT SINKS	24
2.0 Introduction	24
2.1 Governing Equations	26
2.2 Finite Element Formulation	28
2.3 Assembly of Elements and Solution of the Global Matrix	37

CHAPTER THREE : FEM TRAINED ANN MODEL TO PREDICT TWO-PHASE FLOW CHARACTERISTICS IN MICROCHANNELS	40
3.0 Introduction	40
3.1 Governing Equations	40
3.1.1 Conservation of Mass	40
3.1.2 Momentum Balance	42
3.2 Finite Element Formulation	43
3.3 Use of Artificial Neural Networks to Predict Two-Phase Flow Pressure Drops	46
CHAPTER FOUR : ANALYSIS OF SINGLE-PHASE LIQUID COOLED, SINGLE STACK MICROCHANNEL HEAT SINKS	48
4.0 Introduction	48
4.1 Validation of the FEM Model for Thermal Analysis of Microchannel Heat Sinks	53
4.2 Results and Discussions	55
4.2.1 Water Cooled Heat Sinks	55
4.2.1(a) Operation at Low Coolant Flow Rates	55
4.2.1(b) Operation at Higher Coolant Flow Rates	62
4.2.1(c) Effect of Channel Aspect Ratio, Channel Width, Fin Thickness and Material of Construction of the Heat Sink	71
4.2.1(d) Non-Uniform Heating	76
4.2.2 Use of Nanofluids as Coolants	80
CHAPTER FIVE : ANALYSIS OF SINGLE-PHASE LIQUID COOLED, MULTI-STACK MICROCHANNEL HEAT SINKS	86
5.0 Introduction	86
5.1 Validation of the FEM Model for Thermal Analysis	91
5.2 Results and Discussions	93
5.2.1 Operation under Uniform Base Heat Flux and Uniform Coolant Flow Distribution Conditions	93
5.2.2 Effect of Channel Aspect Ratio and Material of the Heat Sink	111
5.2.3 Non-Uniform Heating	116

5.2.3(a) Base Heat Distribution in the Ascending and Descending Orders with respect to the Flow Direction in the Bottom Channel	116
5.2.3(b) Upstream Half Heating, Downstream Half Heating and Centre Half Heating	123
5.2.4 Non-Uniform Coolant Flow Distribution amongst the Heat Sink Stacks	133
5.2.5 Performance Analysis of Multi-Stack Heat Sinks Cooled by Nanofluids	135
CHAPTER SIX : ANALYSIS OF SINGLE STACK MICROCHANNEL HEAT SINKS COOLED BY BOILING TWO-PHASE FLOW	140
6.0 Introduction	140
6.1 Method	143
6.2 Validation of the FEM Model for Thermal Analysis of the Heat Sink with Two-Phase Flow	143
6.3 Results and Discussions	147
6.2.1 Single Stack Heat Sinks Cooled by Boiling Flow of Water	147
6.3.1(b) Preliminary Investigation	147
6.3.1(b) Performance Analysis	148
6.3.1(c) Effect of Heat Dissipation Rate (Q)	160
6.3.1(d) Effect of Coolant Flow Rate	174
6.3.1(e) Effect of Coolant Inlet Pressure	175
6.3.1(f) Non-Uniform Heating	178
6.3.2 Single Stack Heat Sinks Cooled by Boiling Flow of FC-72	181
CHAPTER SEVEN : ANALYSIS OF DOUBLE AND TRIPLE STACK MICROCHANNEL HEAT SINKS COOLED BY BOILING TWO-PHASE FLOW	188
7.0 Introduction	188
7.1 Results and Discussions	188
7.1.1 Multi-Stack Heat Sinks Cooled by Boiling Flow of Water	188
7.1.2 Multi-Stack Heat Sinks Cooled by Boiling Flow of FC-72	204
CHAPTER EIGHT : CONCLUSIONS AND SCOPE FOR FUTURE WORK	208

8.1	Conclusions	208
8.2	Recommendations for Future Work	211
	BIBLIOGRAPHY	212
	APPENDICES	
	Appendix A: MATLAB code Listing for the Analysis of a Typical Liquid Cooled Single Stack Microchannel Heat Sink	219
	Appendix B: Determination of the Coolant Vapor Quality	224
	Appendix C: Determination of the Two-Phase Flow Parameters such as the Two-Phase Friction Multiplier and Void Fraction from the Fem Model explained in Chapter 3	225
	Appendix D: FC-72 Properties	226

LIST OF TABLES

	Page	
1.1	Correlations given by different researchers for the empirical constant C	18
4.1	Node numbers in the order of assembly for the parallel flow heat sink	49
4.2	Node numbers in the order of assembly for the counter flow heat sink	50
4.3	Comparison of thermal resistance obtained by the present method with those obtained by Chong et al. (2002) for a 1 cm x 1cm, single stack, water cooled, counter flow, silicon heat sink of different channel dimensions	55
4.4	Effect of variation of channel aspect ratio, channel width and fin thickness on the thermal and hydraulic performance of a water cooled copper heat sink. Flow rate = 200 ml/min	74
4.5	Thermal resistances for uniform and non-uniform heating of parallel flow heat sink. Flow rate = 200 ml/min	77
4.6	Thermal resistances for uniform and non-uniform heating of counter flow heat sink. Flow rate = 200 ml/min	79
5.1	Node numbers in the order of assembly for a typical double stack parallel flow microchannel heat sink	88
5.2	Node numbers in the order of assembly for a typical double stack counter flow microchannel heat sink	90
5.3	Comparison of thermal resistances obtained by the present method with those obtained by Chong et al. (2002) for water cooled, double stack, counter flow, silicon microchannel heat sinks with different channel dimensions	92
5.4	Comparative thermal resistances of the double stack parallel flow and counter flow water cooled heat sinks for the cases of ascending order heat flux distribution and descending order heat flux distribution (with respect to the coolant flow direction in the bottom channel) and uniform base heating. Flow rate = 100 ml/min	123

5.5	Comparative thermal resistances of the double stack parallel flow and counter flow water cooled heat sinks for the cases of ascending order heat flux distribution and descending order heat flux distribution (with respect to the coolant flow direction in the bottom channel) and uniform base heating. Flow rate = 200 ml/min	124
5.6	Thermal resistances of 1 cm x 1 cm water cooled double stack, parallel flow and counter flow, copper heat sinks ($w = 71 \mu\text{m}$, $Ar = 3$) for different partial heating cases. Flow rate = 100 ml/min. Results are compared with that for uniform heating throughout the base	131
5.7	Thermal resistances of 1 cm x 1 cm water cooled double stack, parallel flow and counter flow, copper heat sinks ($w = 71 \mu\text{m}$, $Ar = 3$) for different partial heating cases. Flow rate = 200 ml/min. Results are compared with that for uniform heating throughout the base	131
5.8	Thermal resistance variation for non-uniform coolant flow amongst the stacks of a double stack, water cooled, copper heat sink with channel dimensions $w = 71 \mu\text{m}$ and $Ar = 3$	134
5.9	Thermal resistance variation for non-uniform coolant flow amongst the stacks of a double stack, water cooled, copper heat sink with channel dimensions $w = 71 \mu\text{m}$ and $Ar = 5$	134
5.10	Thermal resistance variation for non-uniform coolant flow distribution amongst the stacks of a double stack, water cooled, silicon heat sink with channel dimensions $w = 71 \mu\text{m}$ and $Ar = 3$	135
5.11	Thermal resistance variation for non-uniform coolant flow distribution amongst the stacks of a double stack, water cooled, silicon heat sink with channel dimensions $w = 71 \mu\text{m}$ and $Ar = 5$	135
5.12	Thermal resistances and pumping powers of double stack, parallel flow and counter flow copper microchannel heat sinks cooled by Cu-Water nanofluid. Comparative thermal and hydraulic performances of similar double stack water cooled heat sinks, single stack nanofluid cooled heat sink and single stack water cooled heat sink are also provided. The heat sink configurations are $L = 1\text{cm}$, $B = 1\text{cm}$, $w = 71 \mu\text{m}$, $t = 71 \mu\text{m}$, $Ar = 6$	136
6.1	Fluid surface parameter values (F_{FI}) recommended by Kandlikar and Balasubramanian (2003)	142

6.2	Comparison of the performances of a 15 mm x 15 mm copper heat sink cooled by boiling flow of water for two different microchannel dimensions. Total coolant flow rate = 20 ml/min and $T_{fi} = 60\text{ }^{\circ}\text{C}$, $Q = 350\text{ W}$, $P_o = 1\text{ atm}$	148
-----	---	-----

LIST OF FIGURES

	Page	
1.1	Typical single stack parallel flow microchannel heat sink with rectangular cross section channels	5
1.2	Typical single stack counter flow microchannel heat sink with rectangular cross section channels	5
1.3	Typical multi-stack parallel flow microchannel heat sink with rectangular cross section channels	6
1.4	Typical multi-stack counter flow microchannel heat sink with rectangular cross section channels	6
2.1	The 12 noded finite element used for the discretization of parallel flow microchannel heat sinks	25
2.2	The 12 noded finite element used for the discretization of counter flow microchannel heat sinks	25
2.3	Typical bilinear rectangular finite element	29
2.4	Linear two noded finite element	30
2.5	Flow chart listing the various steps involved in the thermal analysis of a typical liquid cooled single stack microchannel heat sink	39
3.1	Figure 3.1: Schematic of the discretized two-phase coolant flow through the microchannel. Two noded linear (one-dimensional) finite elements are used for discretization.	43
4.1	Typical assembly of elements in the stream-wise direction for single stack parallel flow heat sink	49
4.2	Typical assembly of elements in the stream-wise direction for single stack counter flow heat sink	50
4.3	Thermal resistances at different flow rates for a water cooled, parallel flow, single stack, copper heat sink of dimension 1cm x 1cm	54

4.4	Microchannel base temperature distribution in the stream-wise direction for water cooled, single layer, parallel flow, copper heat sink at a flow rate of 20 ml/min	58
4.5	Microchannel base temperature distribution in the stream-wise direction for water cooled, single layer, counter flow, copper heat sink at a flow rate of 20 ml/min	59
4.6	Increase in base temperature with respect to the coolant inlet temperature at different base heat fluxes for parallel flow and counter flow heat sinks	60
4.7	Pressure drop of the microchannel heat sink for water flow rate of 20 ml/min at different base heat fluxes	61
4.8	Pumping power of the microchannel heat sink for different base heat fluxes at a water flow rate of 20 ml/min	61
4.9	Microchannel base temperature distribution in the stream-wise direction for parallel flow heat sink at different total coolant flow rates ranging from 50 ml/min to 250 ml/min and with a uniform base heat flux of 100 W/cm ²	63
4.10	Microchannel base temperature distribution in the stream-wise direction for parallel flow heat sink at different total coolant flow rates ranging from 50 ml/min to 250 ml/min and with a uniform base heat flux of 100 W/cm ²	64
4.11	Microchannel base temperature distribution in the stream-wise direction for counter flow heat sink at different total coolant flow rates ranging from 50 ml/min to 250 ml/min and with a uniform base heat flux of 100 W/cm ²	65
4.12	Microchannel base temperature distribution in the stream-wise direction for counter flow heat sink at different total coolant flow rates ranging from 50 ml/min to 250 ml/min and with a uniform base heat flux of 200 W/cm ²	66
4.13	Peak microchannel base temperature at different coolant flow rates for a base heat flux of 100 W/cm ²	67
4.14	Peak microchannel base temperature at different coolant flow rates for a base heat flux of 200 W/cm ²	67
4.15	Thermal resistance variation with flow rate for parallel flow copper heat sink for two different base heat fluxes	68
4.16	Thermal resistance variation with flow rate for counter flow heat sink. The corresponding thermal resistances of the parallel flow heat sink are added for the sake of comparison	69
4.17	Variation of Pressure drop with coolant flow rate	70
4.18	Variation of pumping power with coolant flow rate	70

4.19	Variation of heat sink thermal resistance with channel aspect ratio	71
4.20	Variation of pressure drop with channel aspect ratio	73
4.21	Variation of pumping power with channel aspect ratio	73
4.22	Microchannel base temperature distribution in the stream-wise direction for non-uniform heating of parallel flow heat sink of dimension 1cm x 1 cm. Results are compared with that for uniform heating	77
4.23	Microchannel base temperature distribution in the stream-wise direction for non-uniform heating of counter flow heat sink of dimension 1cm x 1 cm. Results are compared with that for uniform heating	79
4.24	Thermal resistance variation of a water-Cu nanofluid cooled, parallel flow microchannel heat sink of dimensions 1cm x1cm	84
4.25	Thermal resistance variation of a water-Cu nanofluid cooled, counter flow microchannel heat sink of dimensions 1cm x1cm	84
4.26	Pressure drop variation of a water-Cu nanofluid cooled, microchannel heat sink of dimensions 1cm x1cm	85
5.1	Typical assembly of elements and node numbering for a double stack parallel flow microchannel heat sink	87
5.2	Typical assembly of elements and node numbering for a double stack counter flow microchannel heat sink	89
5.3	Variation of thermal resistance with the number of heat sink stacks. The pressure drop is fixed at 0.1 bar. All the thermal resistances are normalized to the case of single stack heat sink.	91
5.4	Base temperature distributions along the microchannel length for parallel flow and counter flow heat sinks with different number of stacks ranging from 1 to 5. Coolant flow rate = 100 ml/min	96
5.5	Base temperature distributions along the microchannel length for parallel flow and counter flow heat sinks with different number of stacks ranging from 1 to 5. Coolant flow rate = 150 ml/min	97
5.6	Base temperature distributions along the microchannel length for parallel flow and counter flow heat sinks with different number of stacks ranging from 1 to 5. Coolant flow rate = 200 ml/min	98

5.7	Variation of the coolant and microchannel temperatures along the channel length in a counter flow, double stack, copper heat sink for a total flow rate of 100 ml/min	99
5.8	Variation of the coolant and microchannel temperatures along the channel length in a counter flow, triple stack, copper heat sink for a total flow rate of 100 ml/min	100
5.9	Variation of the coolant and microchannel temperatures of a counter flow, double stack, copper heat sink for a total flow rate of 200 ml/min	101
5.10	Variation of the coolant and microchannel temperatures along the channel length in a counter flow, triple stack, copper heat sink for a total flow rate of 200 ml/min	102
5.11	Variation of the coolant and microchannel temperatures along the channel length in a parallel flow, double stack, copper heat sink for a total flow rate of 100 ml/min	103
5.12	Variation of the coolant and microchannel temperatures along the channel length in a parallel flow, triple stack, copper heat sink for a total flow rate of 100 ml/min	104
5.13	Effect of channel stacking on the thermal resistance of the heat sink with both parallel flow and counter flow arrangements for a flow rate of 100 ml/min	105
5.14	Effect of channel stacking on the thermal resistance of the heat sink with both parallel flow and counter flow arrangements for a flow rate of 150 ml/min	106
5.15	Effect of channel stacking on the thermal resistance of the heat sink with both parallel flow and counter flow arrangements for a flow rate of 200 ml/min	106
5.16	Variation of pressure drop with the number of heat sink stacks for a total flow rate of 100 ml/min	108
5.17	Variation of pressure drop with the number of heat sink stacks for a total flow rate of 150 ml/min	108
5.18	Variation of pressure drop with the number of heat sink stacks for a total flow rate of 200 ml/min	109
5.19	Variation of pumping power with the number of heat sink stacks for a total flow rate of 100 ml/min	109
5.20	Variation of pumping power with the number of heat sink stacks for a total flow rate of 150 ml/min	110
5.21	Variation of pumping power with the number of heat sink stacks for a total flow rate of 200 ml/min	110

5.22	Variation of thermal resistance with number of stacks for a parallel flow copper heat sink at three different channel aspect ratios viz. 3, 4 and 5. Flow rate = 200 ml/min	112
5.23	Variation of thermal resistance with number of stacks for a counter flow copper heat sink at three different channel aspect ratios viz. 3, 4 and 5. Flow rate = 200 ml/min	112
5.24	Variation of thermal resistance with number of stacks for a parallel flow silicon heat sink at three different channel aspect ratios viz. 3, 4 and 5. Flow rate = 200 ml/min	113
5.25	Variation of thermal resistance with number of stacks for a counter flow silicon heat sink at three different channel aspect ratios viz. 3, 4 and 5. Flow rate = 200 ml/min	113
5.26	Variation of pressure drop with number of layers for heat sinks with different channel aspect ratios viz. 3, 4 and 5. Flow rate = 200 ml/min	115
5.27	Variation of pressure drop with number of layers for heat sinks with different channel aspect ratios viz. 3, 4 and 5. Flow rate = 200 ml/min	115
5.28	Section of the microchannel showing base heat flux distribution in ascending order with respect to the flow direction in the bottom channel	117
5.29	Section of the microchannel showing base heat flux distribution in descending order with respect to the flow direction in the bottom channel	117
5.30	Section of the microchannel showing uniform base heat flux distribution	117
5.31	Microchannel base temperature distribution of parallel flow, double stack copper heat sink for the cases of ascending order, descending order and uniform heat flux distributions. Flow rate = 100 ml/min	119
5.32	Microchannel base temperature distribution of parallel flow, double stack copper heat sink for the cases of ascending order, descending order and uniform heat flux distributions. Flow rate = 200 ml/min	120
5.33	Microchannel base temperature distribution of counter flow, double stack copper heat sink for the cases of ascending order, descending order and uniform heat flux distributions. Flow rate = 100 ml/min	121

5.34	Microchannel base temperature distribution of counter flow, double stack copper heat sink for the cases of ascending order, descending order and uniform heat flux distributions. Flow rate = 200 ml/min	122
5.35	Section of the microchannel showing upstream half heating (with respect to the flow direction in the bottom channel)	124
5.36	Section of the microchannel showing downstream half heating (with respect to the flow direction in the bottom channel)	124
5.37	Section of the microchannel showing center half heating	125
5.38	Section of the microchannel showing uniform heating throughout the base	125
5.39	Base temperature distribution for center half heating, upstream half heating and downstream half heating of a 1 cm × 1 cm water cooled, double stack, parallel flow, copper heat sink for a total coolant flow rate of 100 ml/min.	127
5.40	Base temperature distribution for center half heating, upstream half heating and downstream half heating of a 1 cm × 1 cm water cooled, double stack, parallel flow, copper heat sink for a total coolant flow rate of 200 ml/min.	128
5.41	Base temperature distribution for center half heating, upstream half heating and downstream half heating (with respect to the flow in the bottom channel) of a 1 cm × 1 cm water cooled, double stack, parallel flow, copper heat sink for a total coolant flow rate of 100 ml/min.	129
5.42	Base temperature distribution for center half heating, upstream half heating and downstream half heating (with respect to the flow in the bottom channel) of a 1 cm × 1 cm water cooled, double stack, parallel flow, copper heat sink for a total coolant flow rate of 200 ml/min.	130
5.43	Variation of the coolant and microchannel temperatures along the channel length in a water cooled counter flow, double stack, copper heat sink of aspect ratio 6.	138
5.44	Variation of the coolant and microchannel temperatures along the channel length in a nanofluid cooled counter flow, double stack, copper heat sink of aspect ratio 6.	139
6.1	Comparison of wall temperature distributions obtained by the present FEM method with those obtained by Zhang et al. (2002) for two-phase flow of water in a single-microchannel device at two heat power levels viz. 1.32 W and 2.12 W	144

6.2	Variation of thermal conductance with channel width of a 25 mm x 25 mm silicon heat sink for 200 W heat dissipation	146
6.3	Base temperature distribution of the parallel flow and counter flow heat sinks cooled by boiling flow of water for 350 W base heat dissipation and 25 °C coolant inlet temperature	152
6.4	Base temperature distribution of the parallel flow and counter flow heat sinks cooled by boiling flow of water for 350 W base heat dissipation and 40 °C coolant inlet temperature	153
6.5	Base temperature distribution of the parallel flow and counter flow heat sinks cooled by boiling flow of water for 350 W base heat dissipation and 60 °C coolant inlet temperature	154
6.6	Base temperature distribution of the parallel flow and counter flow heat sinks cooled by boiling flow of water for 350 W base heat dissipation and 80 °C coolant inlet temperature	155
6.7	Base temperature distribution of the parallel flow and counter flow heat sinks cooled by boiling flow of water for 350 W base heat dissipation and coolant entry at saturation temperature	156
6.8	Thermal resistances of the parallel flow and counter flow heat sinks cooled by boiling flow of water at different coolant inlet temperatures ranging from 25 °C to coolant saturation temperature at inlet pressure	157
6.9	Pressure drop of the microchannel heat sink cooled by boiling flow of water at different coolant inlet temperatures	158
6.10	Pumping power for the heat sink at different water inlet temperatures	159
6.11	Base temperature distribution of the parallel flow and counter flow heat sinks cooled by boiling flow of water for 200 W base heat dissipation and 25 °C coolant inlet temperature	161
6.12	Base temperature distribution of the parallel flow and counter flow heat sinks cooled by boiling flow of water for 200 W base heat dissipation and 40 °C coolant inlet temperature	162
6.13	Base temperature distribution of the parallel flow and counter flow heat sinks cooled by boiling flow of water for 200 W base heat dissipation and 25 °C coolant inlet temperature	163
6.14	Base temperature distribution of the parallel flow and counter flow heat sinks cooled by boiling flow of water for 200 W base heat dissipation and 80 °C coolant inlet temperature	164
6.15	Base temperature distribution of the parallel flow and counter flow heat sinks cooled by boiling flow of water for 200 W base heat dissipation and coolant entry at saturation temperature	165

6.16	Base temperature distribution of the parallel flow and counter flow heat sinks cooled by boiling flow of water for 450 W base heat dissipation and 25 °C coolant inlet temperature	166
6.17	Base temperature distribution of the parallel flow and counter flow heat sinks cooled by boiling flow of water for 450 W base heat dissipation and 40 °C coolant inlet temperature	167
6.18	Base temperature distribution of the parallel flow and counter flow heat sinks cooled by boiling flow of water for 450 W base heat dissipation and 60 °C coolant inlet temperature	168
6.19	Base temperature distribution of the parallel flow and counter flow heat sinks cooled by boiling flow of water for 450 W base heat dissipation and 80 °C coolant inlet temperature	169
6.20	Base temperature distribution of the parallel flow and counter flow heat sinks cooled by boiling flow of water for 450 W base heat dissipation and coolant entry at saturation temperature	170
6.21	Thermal resistance variation of the parallel flow heat sink cooled by boiling flow of water for different base heat fluxes at different coolant inlet temperatures	172
6.22	Pressure drop variation of the heat sink cooled by boiling flow of water for different base heat fluxes at various coolant inlet temperatures	173
6.23	Pumping power of the heat sink cooled by boiling flow of water for different base heat fluxes at various coolant inlet temperatures	174
6.24	Thermal resistances of parallel flow and counter flow heat sinks cooled by boiling flow of water at different coolant flow rates	175
6.25	Thermal resistances of parallel flow and counter flow heat sinks cooled by boiling flow of water at different coolant inlet pressures	176
6.26	Pressure drops of the heat sink cooled by boiling flow of water at different coolant inlet pressures	177
6.27	Pumping powers of the heat sink cooled by boiling flow of water at different coolant inlet pressures	177
6.28	Microchannel base temperature distribution in the stream-wise direction for a non-uniform heating case wherein, larger amount of heat is concentrated on the upstream half of the channel. The corresponding pressure drop and thermal resistance of the heat sink are also indicated	179

6.29	Microchannel base temperature distribution in the stream-wise direction for a non-uniform heating case wherein, larger amount of heat is concentrated on the downstream half of the channel. The corresponding pressure drop and thermal resistance of the heat sink are also indicated	180
6.30	Base temperature distribution in the stream-wise direction for a 15mm x 15mm copper heat sink cooled by boiling flow of FC-72 with saturated coolant entry, at different base heat dissipations ranging from 50 W to 250 W	182
6.31	Heat sink thermal resistances with saturated coolant entry of FC-72 for different base heat dissipations	183
6.32	Pressure drops of the FC-72 cooled heat sink at different values of Q	184
6.33	Pumping powers of the FC-72 cooled heat sink at different values of Q	184
6.34	Base temperature variation in the stream-wise direction for different channel widths for a FC-72 cooled copper heat sink of base dimensions 15mm x 15mm	185
6.35	Thermal resistances of the heat sink cooled by FC-72 for different channel widths	186
6.36	Pressure drops of the heat sink cooled by FC-72 for different channel widths	186
6.37	Pumping powers of the heat sink cooled by FC-72 for different channel widths	187
7.1	Temperature distribution in a double stack parallel flow heat sink cooled by boiling two-phase flow of water with sub-cooled entry at 25°C	189
7.2	Temperature distribution in a double stack parallel flow heat sink cooled by boiling two-phase flow of water with sub-cooled entry at 40°C	190
7.3	Temperature distribution in a double stack parallel flow heat sink cooled by boiling two-phase flow of water with sub-cooled entry at 60°C	191
7.4	Temperature distribution in a double stack parallel flow heat sink cooled by boiling two-phase flow of water with sub-cooled entry at 80°C	192
7.5	Temperature distribution in a double stack parallel flow heat sink cooled by boiling two-phase flow of water with saturated coolant entry	192

7.6	Temperature distribution in a double stack counter flow heat sink cooled by boiling two-phase flow of water with sub-cooled entry at 25°C	194
7.7	Temperature distribution in a double stack counter flow heat sink cooled by boiling two-phase flow of water with sub-cooled entry at 40°C	195
7.8	Temperature distribution in a double stack counter flow heat sink cooled by boiling two-phase flow of water with sub-cooled entry at 60°C	196
7.9	Temperature distribution in a double stack counter flow heat sink cooled by boiling two-phase flow of water with sub-cooled entry at 80°C	197
7.10	Temperature distribution in a double stack counter flow heat sink cooled by boiling two-phase flow of water with saturated coolant entry	198
7.11	Thermal resistances at different coolant inlet temperatures for a 15 mm x 15 mm, parallel flow and counter flow double stack heat sinks cooled by boiling flow of water	199
7.12	Pumping power at different coolant inlet temperatures for the 15 mm x 15 mm double stack heat sink cooled by boiling flow of water	199
7.13	Variation of thermal resistance with number of stacks in the 15 mm x 15mm parallel flow heat sink cooled by boiling flow of water for Q = 350 W and flow rate = 20 ml/min	200
7.14	Variation of thermal resistance with the number of stacks in the 15 mm x 15mm copper counter flow heat sink cooled by two-phase flow of water for Q = 350 W and flow rate = 20 ml/min	201
7.15	Variation of pumping power with number of stacks for a 15 mm x 15 mm heat sink cooled by two-phase flow of water at Q = 350 W and flow rate = 20 ml/min	202
7.16	Temperature distribution in a boiling water cooled double stack, parallel flow, copper heat sink dissipating 1000 W of heat	203
7.17	Base temperature distribution in a 15 mm x 15 mm double stack, parallel flow, copper heat sink cooled by two-phase flow of FC-72 for different base heats	205
7.18	Comparison of peak microchannel base temperatures of the double stack and single stack heat sinks cooled by boiling flow of FC-72	205
7.19	Comparison of thermal resistances of the double stack and single stack heat sinks cooled by boiling flow of FC-72	206

LIST OF SYMBOLS

1.1	A	Area, m ²
1.2	$Ar = \frac{W}{H}$	Channel Aspect ratio
1.3	B	Width of the heat sink, m
1.4	Bo	Boiling number
1.5	Co	Convection number
1.6	C _p	Specific heat at constant pressure, J/kg°C
1.7	$D_h = \frac{2WH}{W + H}$	Hydraulic diameter of the channel, m
1.8	d _s	Size of the nanoparticles
1.9	Fr	Froude number
1.10	f	friction factor
1.11	G	Coolant mass flux, kg/m ² s
1.12	H	Height of the microchannel, m
1.13	h	heat transfer coefficient, W/m ² °C
1.14	h _{tp}	Two phase flow heat transfer coefficient, W/m ² °C
1.15	i	Enthalpy, J/kg
1.16	i _{fg}	Latent heat of vaporization, J/kg
1.17	k	Thermal conductivity of the microchannel material, W/m°C
1.18	k _f	Thermal conductivity of the coolant, W/m°C

1.19	L	Length of the heat sink or the microchannel length, m
1.20	L_e	Length of the finite element, m
1.21	\dot{m}	Mass flow rate of the coolant, kg/s
1.22	N	Number of channels in the heat sink
1.23	Nu	Nusselt number
1.24	Pr	Prandtl number
1.25	P	Pressure, N/m ²
1.26	P_i	Inlet Pressure, N/m ²
1.27	P_o	Outlet Pressure, N/m ²
1.28	Q	Total base heat dissipated by the heat sink, W
1.29	q	Heat flux, W/m ²
1.30	R	Thermal resistance, °C/W
1.31	Re	Reynolds number
1.32	T	Temperature, °C
1.33	T_w	Microchannel Wall Temperature, °C
1.34	T_f	Coolant temperature, °C
1.35	T_{fi}	Coolant inlet temperature, °C
1.36	t	Fin and base thickness of the microchannel, m
1.37	U	Overall heat transfer coefficient, W/m ² °C
1.38	u	Coolant velocity in the Channel, m/s
1.39	u_{gl}	Slip velocity, m/s
1.40	V	Volumetric coolant flow rate, m ³ /s
1.41	w	Width of the microchannel, m
1.42	x	Dryness fraction or Vapor quality

GREEK SYMBOLS

1.1	ΔP	Pressure drop, N/m ²
-----	------------	---------------------------------

1.2	ϕ_l	Two phase friction multiplier
1.3	α	Void fraction
1.4	ρ	Density, kg/m ³
1.5	ν	Mean specific volume of the two-phase flow, m ³ /kg
1.6	\sim	Approximately (Approximate value)

SUBSCRIPTS

1.1	counter	Counter flow heat sink
1.2	cond	Conduction
1.3	conv	Convection
1.4	f	fluid
1.5	fi	Coolant inlet condition
1.6	g	Gas or vapor phase
1.7	Lbw	Left bottom wall of the microchannel element
1.8	Lf	Coolant or fluid in the left channel
1.9	l	Liquid phase
1.10	o	Microchannel outlet condition
1.11	parallel	Parallel flow heat sink
1.12	Rbw	Right bottom wall of the microchannel element
1.13	Rf	Coolant or fluid in the right channel
1.14	sp	Single phase
1.15	sat	Saturation condition
1.16	tp	Two phase flow
1.17	vw	Vertical wall of the microchannel element

LIST OF ABBREVIATIONS

1.1	ANN	Artificial Neural Networks
1.2	CFD	Computational Fluid Dynamics
1.3	FEM	Finite Element Method
1.4	NA	Not Available
1.5	One-D	One Dimensional
1.5	PC	Personal Computer

LIST OF APPENDICES

		Page
1.1	Appendix A: MATLAB code Listing for the Analysis of a Typical Liquid Cooled Single Stack Microchannel Heat Sink	219
1.2	Appendix B: Determination of the Coolant Vapor Quality	224
1.3	Appendix C: Determination of the Two-Phase Flow Parameters such as the Two-Phase Friction Multiplier And Void Fraction from the Fem Model explained in Chapter 3	225
1.4	Appendix D: FC-72 Properties	226

LIST OF PUBLICATIONS & SEMINARS

- 1.1 **Hegde Pradeep**, Seetharamu, K.N., Aswatha Narayana, P.A., Quadir, G. A., Abdullah M.Z. and Zainal, Z.A. (2005). Thermal Analysis of Micro-channel Heat Exchangers with Two Phase Flow using FEM. *Int. J. Num. Methods for Heat & Fluid Flow*. **15(1)**: 43-60.
- 1.2 **Hegde Pradeep**, Seetharamu, K.N., Aswatha Narayana, P.A. and Abdullah Zulkifly. (2005). Two-Phase Stacked Microchannel Heat Sinks for Microelectronics Cooling. *IMAPS-Journal of Microelectronics and Electronic Packaging*. **2(2)**:122-131.
- 1.3 **Hegde Pradeep**, Abdullah, M.Z., Seetharamu, K.N., Aswatha Narayana, P.A. (2005). Counter and Parallel Two-Phase Flow Microchannel Heat Sinks for Electronics Cooling. *International Journal of Heat Exchangers – In Press*.

- 1.4 **Hegde Pradeep**, Abdullah, M.Z., Hassan, A.Y. and Seetharamu, K.N. (2005). Artificial Neural Network Trained One Dimensional FEM Model to Predict Two Phase Flow Characteristics in Mini/Micro Channels. *IJHEX – In Press*.
- 1.5 **Hegde Pradeep**, Seetharamu, K.N., Aswatha Narayana, P.A., Quadir, G. A., Abdullah M.Z. and Zainal, Z.A. Goh, T.J. (2004). Analysis of Two Phase Microchannel Heat Sinks for High Heat Flux Electronics Cooling. *10th International Workshop on Thermal investigations of ICs and Systems*, France, 29 Sept-1 Oct, pp. 235-239.
- 1.6 **Hegde Pradeep**, Seetharamu, K.N., Aswatha Narayana, P.A., Zulkifly Abdullah, Zainal, Z.A., Goh, T. J. (2004). Single and Double Stack Microchannel Heat Sinks with Two-Phase Flow. *6th International Conference on electronic Material and Packaging (EMAP)*, Malaysia (Penang), 5-7 Dec, pp. 379-384.
- 1.7 **Hegde Pradeep**, Seetharamu, K.N., Aswatha Narayana, P.A., Zulkifly Abdullah. (2004). Thermal Analysis of Single Layer Counter Flow Heat Sinks with Two Phase Flow. *6th Electronic Packaging Technology Conference (EPTC)*, Singapore, 8-10 Dec. pp. 559-563.
- 1.8 **Hegde Pradeep**, Seetharamu, K.N., Abdullah, M.Z., Hassan, A.Y. (2006). Multi-Stack Microchannel Heat Sinks with Counter Flow Arrangement for Efficient Electronics Cooling. *18th National & 7th ISHMT-ASME Heat and Mass Transfer Conference*, Guwahati, India, 4 – 6 Jan. pp. 2380-2384
- 1.9 **Hegde Pradeep**, Abdullah, M.Z., Hassan, A.Y., Rajagopal, M.S. and Seetharamu, K.N. (2006). Finite Element Simulation of Multi-Stack Microchannel Heat Sinks with Parallel and Counter Two Phase Flow. *18th National & 7th ISHMT-ASME Heat and Mass Transfer Conference*, IIT Guwahati, India, 4 – 6 Jan. pp. 806-811.

JOURNAL PAPERS UNDER REVIEW

- 1.2 **Hegde Pradeep**, Abdullah, M.Z., Hassan, A.Y. An Improved Finite Element Method to Predict the Thermal Performances of Counter Flow Microchannel Heat Sinks. *IMAPS-Microelectronics International- Under Review*.

PENYERAP HABA SALURAN MIKRO BAGI PENYEJUKAN FLUKS HABA TINGGI PERALATAN ELEKTRONIK – ANALISA DENGAN ALIRAN SATU DAN DUA FASA

ABSTRAK

Penyerap haba saluran mikro menjadikan sebuah teknologi penyejukan berinovatif bagi lesapan berkesan jumlah haba yang besar daripada kawasan yang amat kecil dan terhad bagi cip dan litar elektronik mikro fluks haba yang tinggi. Dalam kajian ini model unsur terhingga umum telah dibina bagi menganalisa penyerap haba saluran mikro yang disejukkan samada aliran satu fasa atau dua fasa. Sebuah unsur terhingga 12 nod telah dibina yang mana boleh digunakan bagi menganalisa pelbagai konfigurasi penyerap haba saluran mikro iaitu satu lapisan dan lapisan berbilang aliran sama arah dan berlawanan arah bagi penyerap haba yang disejukkan oleh cecair satu fasa atau aliran mendidih dua-fasa. Menumpu biasanya didapati lebih kurang 15 unsur terbina per lapisan bagi aliran satu fasa dan dengan lebih kurang 100 unsur bagi aliran dua fasa.

Oleh itu, kaedah ini tidak memerlukan lebih masa komputer berbanding kaedah biasa CFD. Kaedah unsur terhingga yang dibina dalam bahasa Matlab boleh menghasilkan keputusan dalam 20 saat bagi aliran satu fasa dan dalam satu minit bagi dua fasa dengan menggunakan komputer Pentium-4 chipset dan 256 MB RAM. Kaedah ini juga boleh mengendalikan kes haba per luas tak seragam dan aliran cecair penyejuk yang tak seragam. Tambahan pula kaedah satu dimensi dibina untuk menentukan perbezaan tekanan dalam aliran dua fasa dalam penyerap haba. Keputusan yang didapati digunakan untuk melatih artificial network (ANN) yang dilatih boleh digunakan untuk terus menjangka perbezaan tekanan dalam aliran dua fasa.

Didapati daripada kajian bahawa sebuah penyerap haba aliran berlawanan satu lapisan haba memberikan keseragaman suhu lebih baik pada arah aliran dan rintangan

haba yang rendah sebanyak 20% bagi konfigurasi ini, berbanding penyerap haba aliran sama arah yang sama. Kesemua analisa telah dijalankan dengan kuasa pam yang terhad bagi teknologi pam mikro dan mini masa kini. Dengan harapan bagi menghasilkan rintangan terma yang rendah bagi penyerap haba, penyerap haba saluran mikro dianalisa menggunakan penyejuk bendalir nano dan memberikan peratus penurunan dalam rintangan terma.

Juga didapati bahawa penyerap haba lapisan berbilang memberikan rintangan haba rendah yang ketara dan kejatuhan tekanan yang rendah berbanding penyerap satu lapisan. Penyerap haba aliran berlawanan-arah dua lapisan lebih baik daripada penyerap haba aliran sama arah pada kadar aliran yang tinggi dan agihan haba yang seragam memberikan sehingga 15% rendah R bagi konfigurasi yang dikaji. Tambahan, penyerap haba juga dianalisa bagi perbezaan jenis fluks haba di dasar tak seragam dan agihan aliran penyejuk.

Penyerap haba saluran mikro yang disejukkan oleh aliran mendidih dua fasa, memberikan keseragaman suhu yang amat baik dan rintangan terma dan kuasa pam yang amat rendah. Aliran mendidih bagi air dan cecair Fluorinert FC-72 dianalisa. Didapati bahawa bagi jumlah haba terbebas yang diberi bagi penyerap haba aliran dua-fasa menghendaki kuasa pam rendah yang ketara berbanding penyerap haba satu-fasa. Aliran dua-fasa yang disejukkan penyerap haba aliran berlawanan-arah satu lapisan dan aliran dua lapisan yang disejukkan penyerap haba berbilang lapisan juga dianalisa. Didapati bahawa aliran berlawanan-arah penyerap haba memberikan keseragaman suhu yang lebih baik dan lebih daripada 20% lebih rendah rintangan haba, berbanding penyerap haba aliran sama arah bagi konfigurasi yang dikaji. Haba terbebas bagi 1000 W dengan kuasa pam adalah serendah 35 mW telah dihasilkan dengan penyerap haba tersejuk air mendidih dua lapisan.

MICROCHANNEL HEAT SINKS FOR COOLING HIGH HEAT FLUX ELECTRONIC DEVICES—ANALYSIS WITH SINGLE AND TWO PHASE FLOWS

ABSTRACT

Microchannel heat sinks constitute an innovative cooling technology for the efficient dissipation of the large amounts of heat from the very small and constrained areas of the high heat flux microelectronic chips and circuits. In the present study a general finite element model is developed to analyze microchannel heat sinks cooled by either single phase or two-phase flow. A 12 noded finite element is developed, which can be used to analyze a variety of microchannel heat sink configurations viz. single stack and multi-stack parallel and counter flow heat sinks cooled by single phase liquid or boiling two-phase flow. Convergence is typically obtained with about 15 assembled elements per stack for single-phase flow and with about 100 elements for two-phase flow. Consequently the method developed involves considerably less computational effort compared to conventional CFD methods. A MATLAB programme implementing the above FEM model executes within 20 seconds for single phase flow cooled heat sink and within one minute for two-phase flow cooled heat sink on a PC equipped with Pentium-4 chipset and 256 MB RAM. The present method also has the ability to handle cases of non-uniform base heat flux and coolant flow distributions. Additionally, a one dimensional finite element model trained artificial neural network is developed to determine two-phase flow pressure drop in microchannel heat sinks.

It is observed from the study that a single stack counter flow heat sink yield better stream-wise temperature uniformity and lower thermal resistance of the order of 20 % for the configurations considered, than a similar parallel flow heat sink. All the analyses are done within the pumping power constraints of the present day micro and mini pumping technologies. With a view to achieve lower heat sink thermal resistances,

microchannel heat sinks are analyzed using nanofluid coolants and the achievable percentage reduction in thermal resistance is documented.

It is further observed that multi-stack heat sinks yield substantially lower thermal resistance and lower pressure drop than their single stack counterparts. Double stack counter flow heat sinks outperform parallel flow heat sinks at higher flow rates and uniform heat distributions providing upto 15% lower R for the configurations considered. Further, the heat sinks are also analyzed for different kinds of non-uniform base heat flux and coolant flow distributions.

Microchannel heat sinks cooled by boiling two-phase flow yield excellent temperature uniformity and very low thermal resistances and pumping powers. Boiling flow of water and Fluorinert liquid FC-72 are considered for analyses. It is observed that for a given amount of heat removal two-phase flow heat sinks consume considerably less pumping power compared to single-phase cooled heat sinks. Two-phase flow cooled single stack counter flow heat sinks and two-phase flow cooled multi-stack heat sinks are also analyzed. It is observed that counter flow two-phase cooled heat sinks yield better temperature uniformity and more than 20% lower thermal resistances than the parallel flow heat sinks for the configuration considered. Heat dissipations of the order of 1000 W with pumping power as low as 35 mW are demonstrated with double stack boiling water cooled heat sinks.

CHAPTER 1 INTRODUCTION

1.0 Microchannel Heat Sinks for High Heat Flux Electronics Cooling

Thermal management has served as a key enabling technology in the development of advanced microelectronic systems and has facilitated many of the advances in consumer products and modern high-performance computers and microelectronic systems.

The severe urge for greater IC speeds, functionality and miniaturization has fuelled an extraordinary acceleration in chip power dissipation. Amongst all the issues facing chip and computer designers, none is more burning than the soaring levels of power flowing through the integrated circuits. Thermal demands are continuously on the rise. Increasing process speeds (~1.5 GHz), decreasing product sizes and styling requirements cause higher and higher heat loads on the products and consequently thermal management is becoming a critical bottleneck to system performance. Also, the customer demands of lower price and greater reliability are forcing rapid market changes and accelerated product developments. The National Electronic Technology Roadmap, 1997 has affirmed the expectation that the Moore' law improvements in the semiconductor technology will continue into the second decade of the 21st century (Bar-Cohen, 1999). Due to these enhancements, the chip level heat fluxes have gone up tremendously and heat fluxes are expected to fast exceed 100 W/cm² (Phillips, 1990a, Mudawar, 2001, Ross, 2004). High heat fluxes of the order of 10²-10³ W/cm² are also found in opto-electronic equipments, high performance super computers, power devices, electric vehicles and advanced military avionics (Mudawar, 2001). A further challenging aspect is the non-uniform heat flux distribution in electronics. In a high power application such as a server chip the non-uniform heat distribution may lead to

peak heat fluxes which are over 5 times the average heat flux over the entire chip surface.

The performance of electronic system deteriorates precipitously when the temperature of the electronic devices trips beyond a certain threshold limit. The temperature also determines the service life of the electronic equipment. Excessively high temperature degrades the chemical and structural integrity of various materials used in the equipment. Large fluctuations of temperature as well as large spatial variations of temperature in the equipment become responsible for malfunctions and eventual breakdown of the equipment. The purpose of thermal design is to create and maintain throughout the equipment a temperature distribution having limited variations around a moderate level. As a consequence, it is thermal management that often defines the limits of performance, functionality and reliability of electronic devices. Without enhancements in thermal modeling, management and design techniques it is unlikely that the full potential of future semiconductor device technology could be fully realized in product performance and cost effectiveness.

Conventional methods of cooling such as forced convection air-cooling fail to dissipate away the astronomical volumetric heats from the very small surfaces of electronic chips and circuits. The International Technology Roadmap for Semiconductors, 2003 (<http://public.itrs.net>) predicts that the junction-ambient thermal resistance should be reduced to as low as 0.18 °C/W by the year 2010. Under the pressure from these developments, a clear shift from air-cooling technology is needed. Microchannel heat sinks (liquid cooled or two-phase flow cooled) are widely regarded as being amongst the most effective heat removal techniques from the space constrained electronic devices. Apart from providing very high heat transfer coefficients, microchannel heat sinks have the added benefit of being very compact in size, which enhances their suitability to electronics cooling.

The concept of a microchannel heat sink was first introduced by Tuckerman and Pease in 1981 (Tuckerman and Pease, 1981). The potential of handling ultra-high heat fluxes has subsequently resulted in intensive research into microchannel heat sinks (Wu and Little, 1983, Phillips, 1990b, Bowers and Mudawar, 1994a, Bowers and Mudawar, 1994b, Kim and Kim, 1999, Vafai, 1999). A typical microchannel heat sink consists of a number of parallel channels (usually of rectangular cross section) precision cut/chemical etched (Kandlikar and Grande, 2002) directly on the back of the electronic chip (Tuckerman and Pease, 1981) or separately in a metal block of silicon (Wei, 2004), copper (Qu and Mudawar, 2003b) or aluminum (Zhang et al., 2005). The parallel channel dimensions are typically less than 1000 μm (Phillips, 1990b, Qu and Mudawar, 2003b). The top of the heat sink is insulated by a cover and is considered adiabatic. A liquid coolant such as water is pumped through the microchannels of the heat sink so as to extract the heat from the source (electronic chip) on which it is mounted.

The distinctive feature of the microchannel heat sinks is the miniature size of the channels and the fins. The hydraulic diameter of these microchannels may vary from 10 μm to 1000 μm (Qu and Mudawar, 2003b). The need to have micro sized channels arises from the fact that for a fixed temperature difference the heat transfer rate is proportional to the product of the overall heat transfer coefficient U and the heat transfer area A . The large increase in UA can be achieved by increasing the overall heat transfer coefficient U which in turn can be increased by increasing the heat transfer coefficient h . For flow through ducts and tubes large increase in h can be achieved by having very small hydraulic diameters. For instance, fully developed laminar flow of water in a channel of 100 μm hydraulic diameter typically provides a heat transfer coefficient of the order 30,000 $\text{W/m}^2\text{ }^\circ\text{C}$ (Phillips, 1990a). Such large heat transfer coefficients added up with the surface enhancement of the fins would lead to very low thermal resistances typically in the range of 0.1 $^\circ\text{C/W}$ (Phillips, 1990a).

Consequently microchannel heat sinks can dissipate large amounts of heat with minimum temperature rise. This makes microchannel heat sinks ideally suited for cooling the space constrained electronic devices.

Traditionally microchannel heat sinks have been studied for single stack, single-phase flow cooled, parallel flow configurations (Tuckerman and Pease, 1981, Phillips, 1987, Qu and Mudawar, 2002). A single stack parallel flow heat sink as shown in Figure 1.1 has a single layer of parallel channels and the coolant flows in each of the channels in the same direction. However, to attain lower thermal resistances and lower pressure drops several modifications can be made in the flow and heat sink configurations viz. single stack, liquid cooled, counter flow heat sink which has a single layer of parallel channels and the coolant is made to flow in opposite directions through the adjacent channels (Figure 1.2), parallel flow multi-stack heat sinks which have more than one layer of channels stacked one above the other and the coolant flows parallelly in the same direction through all the channels in all the stacks (Figure 1.3) and counter flow multi-stack heat sinks (Figure 1.4) which have more than one layer of channels stacked one above the other and the coolant flows in opposite directions for any given pair of adjacent stacks. It can be noted from Figures 1.2 and 1.4 that the single stack counter flow and multi-stack counter flow heat sinks are operationally different in that the coolant flows in opposite directions through adjacent channels of the same stack in case of the single stack counter flow heat sink whereas, for a multi-stack counter flow heat sink the flow direction is same for the channels of any one given stack but, the flow is opposite with respect to any two adjacent stacks.

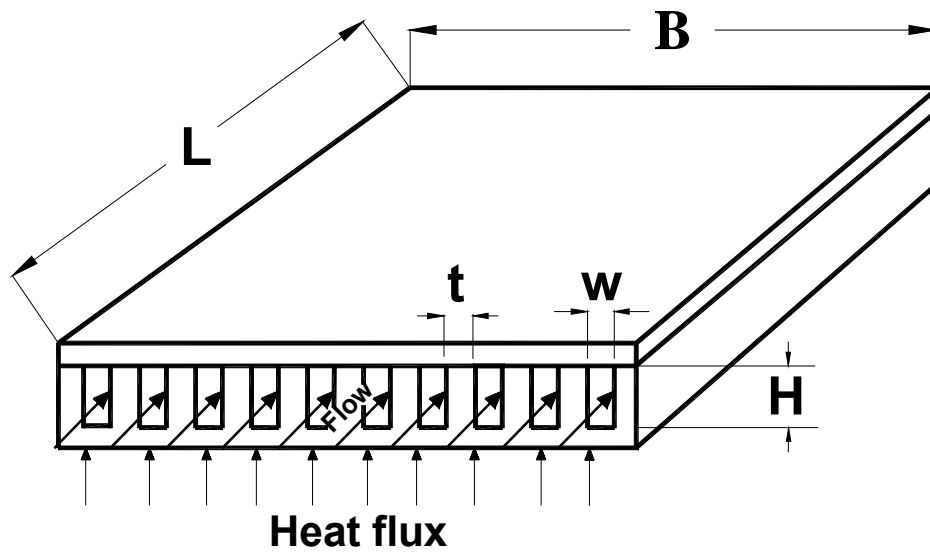


Figure 1.1: Typical single stack parallel flow microchannel heat sink with rectangular cross section channels

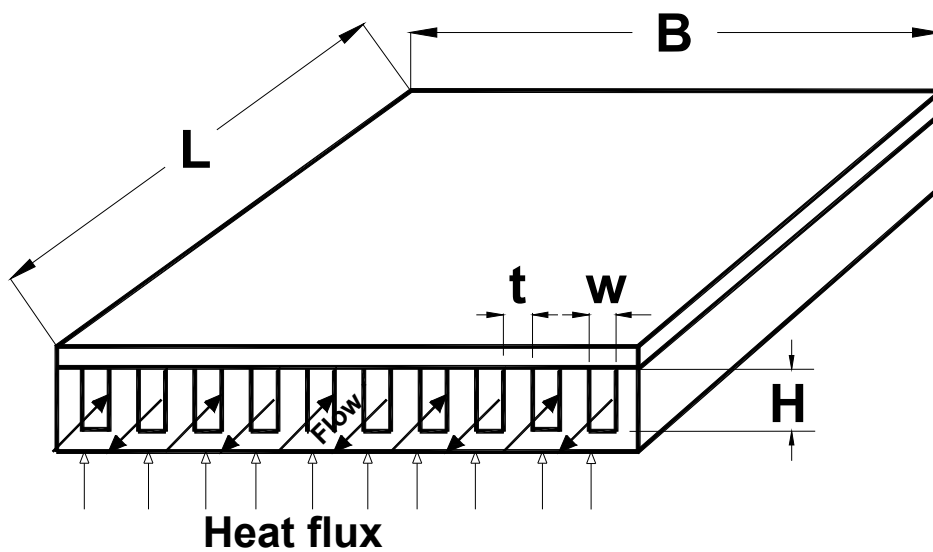


Figure 1.2: Typical single stack counter flow microchannel heat sink with rectangular cross section channels

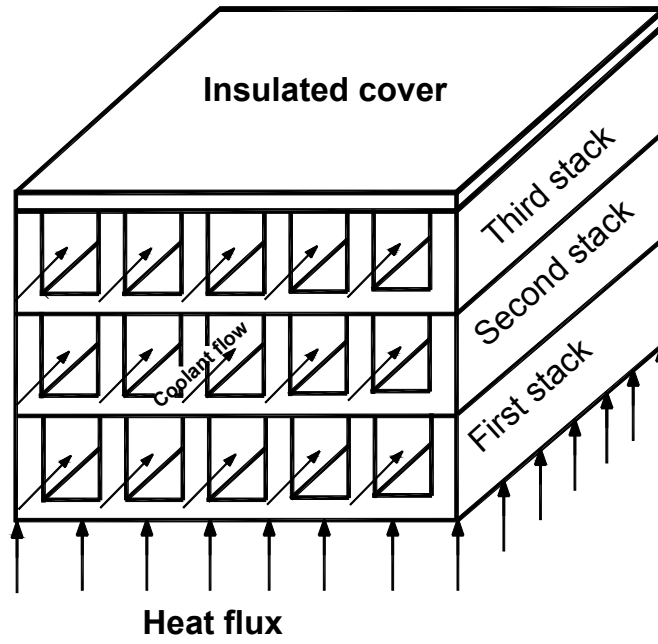


Figure 1.3: Typical multi-stack parallel flow microchannel heat sink with rectangular cross section channels

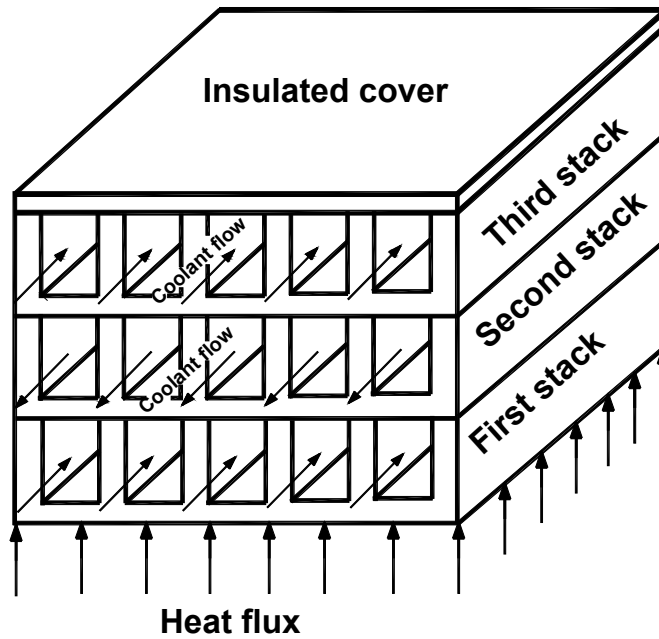


Figure 1.4: Typical multi-stack counter flow microchannel heat sink with rectangular cross section channels

Another attractive option, which is getting considerable attention recently is two-phase flow (boiling flow) cooling in microchannel heat sinks. Two-phase flow cooling have several advantages such as better cooling capability due to higher heat transfer coefficients, ability to handle ultra large heat fluxes of the order of 1000 W/cm^2 and low coolant inventory requirements. Since the interest is recent, the field is very fertile for research. Research is mainly concentrated on the basic aspects of flow and heat transfer in microchannels. Counterflow, single stack heat sinks and stacked heat sinks with two-phase flow are unexplored and the same are simulated in the present work and their performance benefits are documented.

Pressure drop, coolant flow rate and the corresponding pumping powers other important aspects that have to be considered while employing microchannel heat sinks for cooling applications. Microchannel heat sinks with single-phase flow have often been tested and simulated at very high flow rates and pumping powers (Tuckerman and Pease, 1981, Phillips, 1981, Chong et al., 2002) and have been shown to yield low corresponding thermal resistances. But for a microscale application such large pressure drops (of the order of 2.5 bar) and flow rates are not feasible owing to the limitations in micro and mini pumping technologies. It is observed from literature that micropumps (Olsson, 1998, Zeng et al., 2001, Singhal et al., 2004) yield flow rates of the order of 20 ml/min only and maximum pressure drops of the order 2 bar. Slightly larger pumps (minipumps) can be used wherever possible. Annular gear pumps (model No. 7200, 7205, 7223, Micropumps Inc., USA) can be used for this purpose. These pumps measure just 13 mm in diameter and 65 mm in length and can handle flow rates from 4.8 ml/min to 288 ml/min with a maximum differential pressure of 80 bar (http://www.micropump.com/products/pumps/micro_annular/). However, it can be observed that even these pumps can yield maximum flow rates of the order 300 ml/min only. Hence in the present work flow rates are restricted to a maximum of 250 ml/min

only (and pressure drops within 0.5 bar) although, theoretically liquid cooled microchannel heat sinks can perform thermally better at higher flow rates.

Another aspect of importance is the tool for simulating microchannel heat sinks. Traditionally either the Resistance model (Phillips, 1987) or the CFD (Qu and Mudawar, 2002) are used for the analysis. The resistance model is one dimensional and has several shortcomings like inability to handle flow and heat flux non-uniformities. Also, the resistance model cannot be used for analyzing two-phase flow cooled microchannel heat sinks. CFD methods are iterative and computationally very intensive. The present work develops a simple, non-iterative, programmable and general FEM method to thermally analyze single stack and multi-stack microchannel heat sinks with both single-phase flow and two-phase flows with either parallel flow or counter flow arrangements (Hegde et al., 2004, Hegde et al. 2005a, Hegde et al., 2005b, Hegde et al., 2005c, Hegde et al., 2006a). In addition, a one dimensional FEM model is developed to determine two-phase flow pressure drops in microchannel heat sinks (Hegde et al., 2006b). The results from the FEM model are used to train artificial neural networks (ANN) so as to determine two-phase flow pressure drop directly without iterations. Artificial neural networks (ANN) are information processing paradigms that are inspired by the way biological nervous systems process information (Lau, 1992). An artificial neural network is composed of a large number of highly interconnected processing elements called neurons. ANNs have the ability to learn by examples and are configured to a specific application. ANN has two modes of operation the training mode and the using mode. The ANN is first trained with large number of specific inputs and their corresponding outputs. The ANN learns the relation between the inputs and outputs and the trained network can subsequently generate appropriate outputs for completely new values of the input.

1.1 Literature Review

1.1.1 Microchannel Heat Sink Analysis with Single-Phase Flow

Tuckerman and Pease (1981) first demonstrated the use of microchannels for cooling integrated circuits. The channels were fabricated on the back of a silicon substrate. Using water as the coolant and with microchannel dimensions $w = 50 \mu\text{m}$ and $H = 300 \mu\text{m}$, they were able to dissipate heat flux of 790 W/cm^2 for a large pressure drop of the order of 2 bar. The substrate-to-coolant temperature rise was 71°C and the accompanying thermal resistance was 0.1°C/W . Following the pioneering work of Tuckerman and Pease there has been intensive research in the field of microchannel heat sinks owing to their ability to handle ultra high heat fluxes.

The next major contribution to the research on microchannels came from Phillips (1987) who experimentally studied microchannel heat sinks for laminar and turbulent flows. The heat sink was fabricated using indium phosphide and water was used as the coolant. The channel dimensions were typically $w = 220 \mu\text{m}$, $H = 165 \mu\text{m}$ and $L = 9.7 \text{ mm}$. Subsequently a thermal resistance network model to numerically compute the heat sink thermal resistance was developed. Thermal resistances of the order of $0.072^\circ\text{C-cm}^2/\text{W}$ were obtained for very large pressure drops of the order of 2.5 bar.

Peng and Peterson (1995, 1996) experimentally studied the effect of fluid properties and the channel geometry on the convective heat transfer in microchannels. The experimental data showed that the heat transfer is influenced by the temperature of the liquid, Reynolds number and the channel aspect ratio. They proposed correlations to determine Nusselt numbers for laminar and turbulent flow in microchannels.

Copeland (1997) numerically analyzed manifold microchannel heat sinks. The manifold heat sink has many alternating inlet and outlet manifolds that guide the coolant to and from the microchannels and as a result the flow length reduces to a small fraction of the total length of the heat sink. It was found that the manifold heat sinks lead to considerable reduction in pressure drop as the flow length reduced while, channel length shows almost no effect on the thermal resistance. The commercial CFD programme Fluent-4.3.1 was used for the analysis. Thermal resistances of the order of $0.27 \text{ }^\circ\text{C/W}$ were achieved.

Webb and Zhang (1998) experimentally investigated heat transfer and friction characteristics in rectangular microchannels. They observed that the classical correlations were able to predict the single-phase heat transfer coefficient and the friction factor for rectangular channels with reasonable accuracy.

Pfund et al. (1998) measured the pressure drop of water flowing along rectangular microchannels with hydraulic diameters ranging from 200 to 900 μm . In the laminar flow region their data showed good agreement with the conventional theory.

Flockhart and Dhariwal (1998) studied flow of distilled water in trapezoidal channels with hydraulic diameters ranging from 50 to 120 μm and concluded that the theoretical predictions with correlations could predict the friction factors in the channels studied.

Kim and Kim (1999) have modeled microchannel heat sinks as fluid saturated porous medium. The extended Darcy equation proposed by Darcy and Tien (1981) for fluid flow and the volume averaged two-equation model (Tien and Kuo, 1987) for heat transfer are used. An expression for the total thermal resistance was developed after lengthy and tedious simplifications.

Vafai and Zhu (1999) introduced the concept of two layered microchannel heat sinks ($w = 60 \mu\text{m}$, $H = 100 \mu\text{m}$) with counter current arrangement. A three dimensional computational model was developed, a normal case of which ran for about 4 hours on an R-10000 silicon graphic workstation. It was found that the temperature rise of the double stack heat sink is lower compared to the single stack heat sink and at the same time the pressure drop is lower than the single stack heat sink.

Harms et al. (1999) studied single-phase flow in deep rectangular microchannels ($w = 251 \mu\text{m}$, $H = 1000 \mu\text{m}$). Experiments were carried out with distilled water. It was found that for laminar flow the correlation by Shah and London (1978) accurately predicted the Nusselt number. It was further observed that the microchannel system developed for laminar flow outperformed that with turbulent flow, both in terms of flow and heat transfer characteristics.

Qu and Mudawar (2001) studied pressure drop and heat transfer characteristics in copper heat sinks with rectangular microchannels of size $231 \mu\text{m} \times 713 \mu\text{m}$ both experimentally and numerically. Deionized water was used as the coolant. The governing continuity, energy and momentum equations were solved using the SIMPLE algorithm (Patankar, 1980). It was found that at any longitudinal distance along the length of the microchannel the highest temperature is encountered typically at the base surface of the microchannel and the bulk liquid constitutes the region of lowest temperature. Also, no early transition from laminar to turbulent flow in microchannels was observed.

Chong et al. (2002) modelled single layer counter flow and double layer counter flow microchannel heat sinks with rectangular channels. The thermal resistance network was used for modeling. The results were found to be in fairly good agreement with 3-D CFD results obtained from commercial software FLUENT. The microchannel

dimensions were subsequently optimized using a multivariable constrained direct search method by Box (1965). Optimization results showed that both the single layer counter flow and double layer counter flow microchannel heat sinks operating in laminar flow outperform those operating with turbulent flow conditions both thermally and hydrodynamically. However, very large channel aspect ratios viz. 10 and large pressure drops of the order 1.2 bar were considered for optimization. Also, the study does not report the temperature distribution and does not consider heat flux and flow non-uniformities.

Wei and Joshi (2004) analyzed stacked silicon microchannel heat sinks with parallel flow arrangement. The thermal resistance of the heat sink was determined using a one dimensional iterative resistance network. The heat sinks were tested for simple cases of uniform heat flux and flow distributions with fixed pumping power, flow rate and pressure drop. The thermal resistances are normalized to that of the single stack heat sink. Temperature distribution in the heat sink is not reported.

Li et al. (2004) carried out numerical simulation of the heat transfer occurring in silicon based microchannel heat sinks ($w = 57 \mu\text{m}$, $H = 180 \mu\text{m}$) using 3-dimensional conjugate heat transfer model. A finite difference numerical code with a Tri-Diagonal Matrix Algorithm is used to solve the governing equations. The results indicated that the thermophysical properties of the liquid could significantly influence both flow and heat transfer in the microchannel heat sink. A correlation is proposed to calculate the overall averaged Nusselt number for the heat sink.

Lee et al. (2005) experimentally investigated the thermal behaviour of single-phase flow through rectangular copper microchannels. The microchannels considered ranged in widths from $194 \mu\text{m}$ to $534 \mu\text{m}$ with $Ar = 5$. Water is used as the coolant. Numerical simulations were carried out using commercial CFD solver FLUENT so as to

predict mainly the flow Nusselt number. The numerical results were in good agreement with the experimental results.

Zhang et al. (2004) and Zhang et al. (2005) analyzed single stack aluminum microchannel heat sinks ($w = 210 \mu\text{m}$, $Ar = 10$) for liquid cooling of flip chip ball grid array packages. Experiments were carried out with the heat sinks mounted on two different chips with foot prints, 12 mm x 12 mm and 10 mm x 10 mm. A thermal resistance network is used to numerically determine the heat sink thermal resistance at different coolant flow rates. With water cooling, the calculated thermal resistances ranged from 0.44 to 0.32 °C/W for the 12-mm chip case and from 0.59 to 0.44 °C/W for the 10-mm chip case.

Methods to evaluate the single-phase laminar flow pressure drop and the heat transfer coefficients in rectangular ducts have been well documented by Shah and London (1978) and the same have been used successfully by various researchers for microchannel heat sinks with little or no modifications (Phillips, 1990a, Qu and Mudawar 2003a, Chong et al., 2002, Wei and Joshi, 2004, Zhang et a. 2005).

1.1.2 Use of Nanofluids as Coolants

Very limited study regarding the use nanofluids as coolants in micro and mini channel heat sinks exist in literature. Nguyen et al. (2004) have investigated the usage of nanofluids in cooling electronic devices. Water- Al_2O_3 and ethylene glycol- Al_2O_3 nanofluids (with up to 7.5 % nano particle loading) are used in a rectangular slot type macro size heat sink measuring 50 x 50 x 10 mm with a 3 x 48 mm fluid cross section. With nanofluids as the coolant marked reduction in the junction temperature was observed, especially at higher flow rates and higher particle loading percentage. Xuan and Roetzel (2000), Xuan and Li (2003), Maiga et al. (2004) all report that the inclusions of nanoparticles substantially increase the heat transfer performance of the

original base fluid mainly due to the changes in the transport properties of the base fluid and due to the dispersion effects of the nanoparticles in the coolant. However, since the nanoparticles are ultra-fine (<100 nm) and the percentage loading is very less, there is very little difference in the friction characteristics of the nanofluid in comparison to the base fluid. Xuan and Roetzel (2000) and subsequently Xuan and Li (2003) have developed correlations based on their experiments to compute the heat transfer coefficient of nanofluid flow in horizontal tubes.

1.1.3 Microchannel Heat Sink Analysis with Two-Phase Flow

Flow boiling is extensively studied especially in small tubes (of diameter 3 mm and more). However, interests in two-phase flow studies in microchannel heat sinks are rather new and have erupted mainly due to their prospective applications in high flux electronics cooling. Microchannel heat sink studies with two-phase flow are mainly experimental in nature and focus on the basic studies of flow type, determination of heat transfer characteristics etc. Simulation studies with respect to two-phase flow cooled microchannel heat sink performance analyses are very limited.

Bergles and Dorrmer (1969) were amongst the first to perform studies of flow boiling in small tubes with less than 3 mm diameter. They primarily investigated pressure drop associated with flow boiling of water in horizontal tubes of length to diameter ratio 24-195 and diameters 1.57-5.03 mm. The liquid velocity was varied from 1.51 to 18.2 m/s. The inlet temperature was varied from 10 to 62.7 °C and the wall heat fluxes were varied from 0 to 1733.6 W/cm². Their results indicated that for a given inlet velocity and temperature, pressure drop rapidly increases once boiling is well established.

Kandlikar (1990) developed a general correlation for saturated two-phase flow boiling heat transfer inside horizontal and vertical tubes based on a total of 5246 data

points from 24 experimental investigations for about 10 fluids. The proposed correlation gives a 15.9 % mean deviation for all the data for water. Although the Kandlikar correlation was originally developed for macro-sized tubes Kandlikar and Steinke (2002), and Kandlikar and Balasubramanian (2003) have slightly modified the correlation so as to be used for two-phase flow through microchannels.

Wambsganss et al. (1993) have investigated flow boiling of refrigerant R113 in a small circular tube. Their results showed that the flow boiling heat transfer coefficient is a strong function of the applied heat flux (i.e., h_{tp} increases with increasing q keeping all other parameters fixed) and is only weakly dependent on G . They concluded that nucleate boiling is the dominant mode of heat transfer over the range of qualities (0–0.9) tested.

Bowers and Mudawar (1994a, 1994b, 1994c,) performed an experimental study of boiling flow for R-113 flowing through multiport circular channels with hydraulic diameters 2.54 mm and 0.510 mm. This study demonstrated that boiling in narrow channels is an effective method of achieving high heat fluxes, coupled with low flow rates and pressure drops. The homogeneous model (Wallis, 1969, Collier, 1981) was employed to predict the pressure drop in the channel within a deviation of $\pm 30\%$

Tran et al. (1996) have performed nucleate boiling heat transfer studies using a horizontal, rectangular channel with $D_h = 2.40$ mm. They concluded that nucleate boiling was the dominant heat transfer mechanism and for low vapor qualities ($x < 0.3$), h_{tp} was found to decrease with increasing vapor quality. They proposed an empirical correlation where h_{tp} is a function of the boiling number, Weber number and the liquid to vapor density ratio.

Zhang et al. (2002) have conducted flow-boiling experiments for water through single-channel and multi-channel test devices. The channel hydraulic diameter is less than 100 μm . Koo et al. (2001) and Zhang et al. (2002) wrote the heat balance equations for the heat sink and used the finite volume method (Patankar, 1980) to solve the equations. The Kandlikar correlation (Kandlikar, 1990) is used to determine the two-phase flow boiling heat transfer coefficient. The pressure drop was modelled assuming homogenous flow. The two-phase friction coefficient is obtained from an external correlation (Stanley, et al., 1997). It is observed that the simulation results are in fair agreement with the experimental results.

Qu and Mudawar (2003 a, 2003 b) have experimentally studied flow boiling of water in rectangular microchannels of size 231 x 713 μm . Qu and Mudawar (2003 a) studied different empirical correlations for two-phase flow heat transfer coefficient in microchannels and reported that none predict the h_{tp} appropriately. Qu and Mudawar (2003 b) studied different empirical correlations to predict two-phase flow pressure drops in rectangular microchannels. Only the correlation by Mishima and Hibiki (1996) was found to yield acceptable pressure drops (~13% margin of error). Subsequently the provided a new correlation for two-phase flow pressure drops in microchannels (Table 1.1).

Kandlikar and Balasubramanian (2003) and Kandlikar (2004) have compiled new data on flow boiling in microchannels that cover the all-liquid flow Reynolds number between 50-500. The original Kandlikar correlation is slightly modified so as to predict the flow boiling heat transfer in microchannels. The validity of the correlation is well established by comparing the predictions from the modified correlation with the experimental results of different researchers. It is also indicated that the flow boiling is chiefly nucleate boiling dominant in the low Reynolds number range as encountered in microchannels.

Steinke and Kandlikar (2004) have conducted experimental investigation for flow boiling of water in six parallel, horizontal microchannels with a hydraulic diameter of 207 μm . A comparison of the experimental results with the nucleate boiling dominant regime of the Kandlikar flow boiling correlation (Kandlikar, 2004) showed good agreement. They also showed that the modified Kandlikar correlation (Kandlikar, 2004) predicts the right trend of decreasing h_{eff} with increasing vapor quality for two-phase flow through microchannels. Also, it is shown that the Shah and London correlation (1978) can accurately predict the single-phase pressure drop in rectangular microchannels.

Wen and Kening (2004) experimentally investigated two-phase pressure drop during flow boiling of water in a channel with cross section 2 mm by 1mm. The experimental results were compared with four different correlations. Their results indicated that the pressure drops predicted using the Lockhart-Martinelli correlation (Collier, 1980) for two-phase friction multiplier with the modified empirical constant C obtained from Mishima et al. (1996) fits the data with reasonable accuracy while, the correlations by Chisholm (Collier, 1980) and Tran (2000) considerably overpredict the data.

Mishima and Hibiki (1996), Lee and Lee (2001), Qu and Mudawar (2003b) have all experimentally studied two-phase flow in mini mini/micro channels and have provided correlations to predict two-phase flow pressure drop. All the above-mentioned researchers basically use the Lockhart-Martinelli correlation (Collier, 1980) with modified values of the empirical constant C to estimate the two-phase friction multiplier and hence the two-phase pressures drop. The correlations for the empirical constant C as given by Mishima and Hibiki (1995), Lee and Lee (2001), Qu and Mudawar (2003) are given in Table 1.1.

Table 1.1: Correlations given by different researchers for the empirical constant C

Reference	Work	Correlation for the empirical constant C
Lockhart- Martinelli (Collier, 1980)	Study of air-liquid mixtures in large diameter channels (macrochannels)	$C = 5$ for laminar flow
Mishima and Hibiki (1996)	Study of Air-water flow through capillary tubes in the range of 1 to 4 mm.	$C = 21 \left(1 - e^{-0.319 \times 10^3 D_h} \right)$
Lee and Lee (2001)	Study of Air-water flow through horizontal rectangular channels of fixed width 20 mm. The height of the channel varied from 0.4mm to 4 mm	$C = A \lambda^a \psi^r Re_{Lo}^s$ The dimensionless parameters λ , ψ and the constants a , r and s can be obtained from Lee and Lee (2001). Re_{Lo} is the liquid only Reynolds number.
Qu and Mudawar (2003)	Study of flow boiling of water through a heat sink containing 21 parallel microchannels of size 231 x 713 μm .	$C = 21 \left(1 - e^{-0.319 \times 10^3 D_h} \right) (0.00418G + 0.0613)$ where, G is the coolant mass flux.

1.2 Objectives of the Present Work

From the literature review it is clear that there is a need to develop a simple, practical and non-iterative but accurate approach to analyze microchannel heat sinks both in single and two-phase flows. Cases of non-uniform base heating and non-uniform flow distribution amongst the microchannel heat sink stacks need to be studied in greater depth.

Performance analyses of single stack counter flow and multi-stack counter flow microchannel heat sinks need to be carried out and their performances need to be compared with their parallel flow counterparts. Performance analyses of multi-stack microchannel heat sinks cooled by two-phase flow need to be done. Also, most of the work for two-phase flow in microchannels are experimental in nature and mostly deal with the fundamental aspects of flow and heat transfer such as the determination of two-phase flow heat transfer coefficient, flow regimes and flow characteristics. Very few work actually deal with the performance analysis of microchannel heat sinks with two-phase flow. To the best of the author's knowledge there are no works that deal with the performance analysis of two-phase flow cooled single stack counter flow microchannel heat sinks, two-phase flow cooled parallel flow multi-stack heat sinks and two-phase flow cooled counter flow multi-stack heat sinks. Also, there exists a need to develop a methodology to determine the two-phase flow pressure drop and flow characteristics in microchannels using the fundamental equations (of mass and momentum conservation) and without using external correlations for the same.

The **objectives** of the present work are:

- a. To develop a simple, practical and programmable method to analyze both parallel flow and counter flow microchannel heat sinks

- b. To analyze the performance of single stack counter flow heat sinks and compare the same with that of single stack parallel flow heat sinks for both single-phase flow and two-phase flows
- c. To analyze the performance benefits of using nanofluids in microchannel heat sinks
- d. To analyze the performances of parallel flow and counter flow liquid cooled Multi-stack heat sinks.
- e. To determine the performance benefits of employing boiling flow (two-phase flow) cooled microchannel heat sinks.
- f. To study the improvements in the thermal and hydraulic performance of the two-phase flow cooled microchannel heat sinks by employing counter current arrangements and stacked heat sink configurations.
- g. To develop a methodology to determine the two-phase flow pressure drop in microchannels using the fundamental equations (of mass and momentum conservation) and without using external correlations for the same.

1.3 Overview of the Present Work and Organization of the Thesis

Microchannel heat sinks with rectangular cross section channels are analyzed. The finite element method is used to analyze microchannel heat sinks. A general 12 noded finite element is developed to analyze the thermal performance of microchannel heat sinks with both single-phase and two-phase flows. Different channel configurations, flow arrangements and channel stacking are analyzed with a quest to evolve lower thermal resistances and lower pumping power. The same 12 noded element can be used for the analysis of all the above-mentioned cases. Water is considered as the coolant for single-phase analysis (because of its excellent thermal properties). Performance enhancement that is achieved by using nanofluid coolants is also studied. For the two-phase flow analysis fluoro inert liquid FC-72 is considered apart from water, because of its lower boiling temperature (at a given pressure). A one dimensional iterative finite element model is subsequently developed to determine the

two-phase flow pressure drop in the microchannels. The results from the one dimensional model are trained into artificial neural networks so as to obtain the two-phase flow pressure drops directly without iterations.

Chapter 2 introduces the 12 noded finite element used for the microchannel discretization. The governing heat balance equations are written and the complete finite element formulation for the analysis of the heat sink using the 12 noded element is performed.

Chapter 3 develops a one dimensional FEM model to determine the two-phase flow pressure drop in the microchannels without the use of external correlations. Apart from the pressure drop determination the model can also analyze and determine other two-phase flow characteristics like the two-phase friction multiplier and the void fraction. Further, the results obtained from the FEM model are used to train Artificial Neural Networks (ANN) so as to determine the results for different channel dimensions and flow conditions without iterations.

Chapters 4 and 5 deal with the analysis of microchannel heat sinks cooled by single-phase liquid flow.

Chapter 4 analyzes single-phase liquid cooled single-stack microchannel heat sinks. Counter flow heat sinks are studied with a quest to obtain better temperature uniformity and lower thermal resistances (than the parallel flow heat sinks). In this chapter both single stack water cooled parallel flow and counter flow heat sinks are analyzed and their thermal performance compared. Depending upon the available micro and mini pumping technologies both low and higher coolant flow rates are considered. It is shown that the counter flow heat sink yields better thermal performance both in terms of lower thermal resistance and better temperature

uniformity along the heat sink. Parametric studies are performed to analyze the effects of channel dimensions, heat flux, flow rate, material of heat sink construction and non-uniform heat flux distributions. Finally performance enhancement that can be achieved using nanofluid coolants is studied.

Chapter 5 discusses the effect of stacking on the thermal and hydraulic performance of the microchannel heat sinks. Parallel and counter flow stacked heat sinks are analyzed and compared and the effects of non-uniformities in the base heat flux and coolant flow distribution are studied.

Chapters 6 and 7 deal with the analysis of single component two-phase flow cooled microchannel heat sinks.

Chapter 6 discusses the analysis of single stack microchannel heat sinks with boiling flow of water and FC-72. It is shown that under similar operating conditions a two-phase flow cooled heat sink yields substantially lower thermal resistance and excellent temperature uniformity compared to a similar single-phase liquid cooled heat sink. It is also shown that counter flow heat sinks with two-phase flow yield comparatively lower thermal resistance and better temperature uniformity than the parallel flow heat sinks. Parametric studies are performed to study the effects of heat dissipation rates, coolant inlet temperature, coolant inlet pressure and flow rate. Trained artificial neural network is used to determine the two-phase flow pressure drop in the microchannels. It is further shown that lower microchannel base temperatures can be obtained by employing boiling flow of FC-72 as the coolant.

Chapter 7 studies the performance of parallel flow and counter flow stacked heat sinks with two-phase flow. It is observed that stacked heat sinks cooled by two-phase flow yield lower thermal resistances and lower pressure drops compared to their

single-stack counterparts. The performance benefits in terms of thermal resistance and pressure drop are reported.

Chapter 8 presents the conclusions of the present work and discusses the scope for future work.

CHAPTER 2 FINITE ELEMENT MODEL FOR THERMAL ANALYSIS OF MICROCHANNEL HEAT SINKS

2.0 Introduction

Microchannel heat sinks with rectangular cross section channels are analyzed. Taking advantage of the symmetry a single pair of adjacent channels of the heat sink is considered for analysis. A twelve noded, repetitive finite element representing a pair of adjacent microchannels is used for the finite element modeling. A typical element used for the discretization of parallel flow heat sink is shown in Figure 2.1. Nodes 5 and 6 of the element represent the coolant flow in the left channel while the nodes 9 and 10 represent the coolant flow in the adjacent right channel. Nodes 2-3-7-8 represent the dividing wall between two channels while, nodes 1-2-3-4 and 2-11-12-3 represent the left and right bottom walls respectively. The element as a whole is actually an assembly of four noded bilinear rectangular elements and two noded linear elements. The microchannel bottom and dividing walls are constituted by the bilinear rectangular elements while, the coolants are discretized by two noded linear elements, the two fluid nodes being located at the inlet and the outlet of the overall cell. The base of the microchannel receives heat from the source and the heat is transferred to the coolant by convection directly from the base and indirectly through the dividing wall. The entire element is repeatable in the sense that suitable number of elements can be assembled in the length-wise and lateral directions to constitute a complete microchannel heat sink. Similar element with the coolant flow directions in the adjacent channels being opposite to one another (Figure 2.2) is used for the discretization of the single layer counter flow heat sinks. The elements can be assembled in the stream-wise direction i.e. along the flow direction or length of the channel so as to represent a complete microchannel. The assemblies of elements for different kinds of heat sink configurations are shown in figures 4.1, 4.2 and 5.1 and 5.2 respectively.